High-Pressure NMR Kinetics, Part 95[+]

Solution and Solid-State Characterization of Eu^{II} Chelates: A Possible Route Towards Redox Responsive MRI Contrast Agents

László Burai, Éva Tóth, Sabine Seibig, Rosario Scopelliti, and André E. Merbach*[a]

Abstract: We report the first solid state X-ray crystal structure for a Eu^{II} chelate, $[C(NH_2)_3]_3[Eu^{II}(DTPA)(H_2O)]\cdot 8H_2O$, in comparison with those for the corresponding Sr analogue, $[C(NH_2)_3]_3[Sr(DTPA)(H_2O)]\cdot 8H_2O$ and for $[Sr(ODDA)]\cdot 8H_2O$ ($DTPA^{5-}$ = diethylenetriamine-*N*,*N*,*N*′,*N*″,*N*″-pentaacetate, $ODDA^{2-}$ = 1,4,10,13-tetraoxa-7,16-diazacyclooctadecane-7,16-diacetate). The two DTPA complexes are isostructural due to the similar ionic size and charge of Sr^{2+} and Eu^{2+}. The redox stability of $[Eu^{II}(ODDA)(H_2O)]$ and $[Eu^{II}(ODDM)]^{2-}$ complexes has been investigated by cyclovoltammetry and UV/Vis spectrophotometry ($ODDM^{4-}$ = 1,4,10,13-tetraoxa-7,16-diaza-cyclooctadecane-7,16-dimalonate). The macrocyclic complexes are much more stable against oxidation than $[Eu^{II}(DTPA)(H_2O)]^{3-}$ (the redox potentials are $E_{1/2} = -0.82$ V, -0.92 V, and -1.35 V versus Ag/AgCl electrode for $[Eu^{III/II}(ODDA)(H_2O)]$, $[Eu^{III/II}(ODDM)]$, and $[Eu^{III/II}(DTPA)(H_2O)]$, respectively, compared with -0.63 V for $Eu^{III/II}$ aqua). The thermodynamic stability constants of $[Eu^{II}(ODDA)(H_2O)]$, $[Eu^{II}(ODDM)]^{2-}$, $[Sr(ODDA)(H_2O)]$, and $[Sr(ODDM)]^{2-}$ were also determined by pH potentiometry. They are slightly higher for the Eu^{II} complexes than those for the corresponding Sr analogues ($\log K_{ML} = 9.85$, 13.07, 8.66, and 11.34 for $[Eu^{II}(ODDA)(H_2O)]$, $[Eu^{II}(ODDM)]^{2-}$, $[Sr(ODDA)(H_2O)]$, and $[Sr(ODDM)]^{2-}$, respectively, 0.1M $(CH_3)_4NCl$). The increased thermodynamic and redox stability of the Eu^{II} complex formed with ODDA as compared with the traditional ligand DTPA can be of importance when biomedical application is concerned. A variable-temperature ^{17}O-NMR and ^1H-nuclear magnetic relaxation dispersion (NMRD) study has been performed on $[Eu^{II}(ODDA)(H_2O)]$ and $[Eu^{II}(ODDM)]^{2-}$ in aqueous solution. $[Eu^{II}(ODDM)]^{2-}$ has no inner-sphere water molecule which allowed us to use it as an outer-sphere model for $[Eu^{II}(ODDA)(H_2O)]$. The water exchange rate ($k_{ex}^{298} = 0.43 \times 10^9\ s^{-1}$) is one third of that obtained for $[Eu^{II}(DTPA)(H_2O)]^{3-}$. The variable pressure ^{17}O-NMR study yielded a negative activation volume, $\Delta V^{\neq} = -3.9\ cm^3 mol^{-1}$; this indicates associatively activated water exchange. This water exchange rate is in the optimal range to attain maximum proton relaxivities, which are, however, strongly limited by the fast rotation of the small molecular weight complex.

Keywords: contrast agents · europium(II) complexes · lanthanides · magnetic resonance imaging · NMR spectroscopy · water exchange

Introduction

Complexes of divalent europium have recently received a growing interest, which originates from two aspects. The ionic radius of Eu^{II} is between those of the Ca^{II} and Sr^{II} ion (ionic radii are 125, 112, and 126 pm for Eu^{II}, Ca^{II}, and Sr^{II}, respectively)[2] and its chemical properties—except for the redox behavior—also show similarity with those of the alkaline earth metal ions. Therefore, the Eu^{II} ion was proposed as a spectroscopic probe of Ca^{II} in biological systems.[3] Furthermore, Eu^{II} has seven unpaired electrons in an ^8S ground state and is isoelectronic with Gd^{III}. In the last two decades, Gd^{III} poly(amino carboxylate) complexes have been successfully used in medical diagnostics as contrast agents in magnetic resonance imaging and were intensively investigated both for their electronic relaxation and water exchange properties which influence their efficiency.[4–5]

[a] Prof. A. E. Merbach, Dr. L. Burai, Dr. É. Tóth, Dr. S. Seibig, Dr. R. Scopelliti
Institut de Chimie Minérale et Analytique
Université de Lausanne-BCH, 1015 Lausanne (Switzerland)
Fax: (+41) 21-692-3875
E-mail: andre.merbach@icma.unil.ch

Supporting information for this contribution is available on the WWW under http://www.wiley-vch.de/home/chemistry/. The following supporting information is available: X-ray structure of $[Sr(DTPA)(H_2O)]^{3-}$ (Figure S1), UV/Vis spectrum of $[Eu^{II}(ODDA)(H_2O)]$ and $[Eu^{II}(ODDM)]^{2-}$ (Figures S2a and S2b), species distribution diagram of the Sr^{2+}-$ODDM^{4-}$ and Sr^{2+}-$ODDA^{2-}$ systems (Figures S3a and S3b), data for X-ray structures (Tables S1–S4), variable-temperature reduced transverse and longitudinal ^{17}O relaxation rates and chemical shifts of $[Eu^{II}(ODDA)(H_2O)]$ and $[Eu^{II}(ODDM)]^{2-}$ solution (Table S5 and S6), reduced transverse ^{17}O relaxation rates as a function of pressure for $[Eu^{II}(ODDA)(H_2O)]$ (Table S7), and proton relaxivities as a function of the magnetic field (Table S8 and S9).

[+] For Part 94, see ref. [1].

Studying appropriate complexes of the isoelectronic Eu^{II} may give deeper insight into those processes of Gd^{III} and open new ways in the field of developing specific redox responsive contrast agents.

Nowadays there is an increasing demand for NMR-sensitive probes of a specific property of the biological environment. Special attention is devoted to systems able to probe changes in pH, temperature, or partial oxygen pressure. Assessment of pO_2 changes can be of high importance in many cases, such as the differentiation between venous and arterial blood, pathological states associated with stroke, tumors or cerebral mapping of task activation. Redox, or more particularly pO_2 responsive contrast agents can be imagined with complexes where the metal can switch between oxidation states characterized by different relaxation properties. Beside manganese(III/II) which has been proposed recently,[6] europium(III/II) chelates can also be good candidates, provided the stabilization of the lower oxidation state is controlled. Certainly, the development of applicable pO_2 responsive agents requires a strong biochemical expertise as well, but as a first step, the exploration of basic chemistry of the possible systems is primordial.

We have recently investigated the water exchange kinetics and electronic relaxation on the Eu^{II} aqua[7–8] and the $[Eu^{II}(DTPA)(H_2O)]^{3-}$ complexes[9] ($DTPA^{5-}$ = diethylenetriamine-*N*,*N*,*N*′,*N*″,*N*″-pentaacetate). The water exchange of the Eu^{II} aqua complex was found to be the fastest ever measured by magnetic resonance, while its electronic relaxation was slower compared with the isoelectronic Gd^{III} aqua ion. Unfortunately, the redox stability of Eu^{II} poly(amino carboxylates) in aqueous solution is lower than that of the Eu^{II} aqua complex, which raised difficulties when investigating for example, $[Eu^{II}(DTPA)(H_2O)]^{3-}$. Therefore, our objective was to find other Eu^{II} poly(amino carboxylate) complexes with higher redox stability in aqueous solution. Although a lot is known about the preparation, optical and electrochemical properties of aqueous solutions of Eu^{II} inorganic salts,[10] only few data are available on Eu^{II} poly(amino carboxylates).[11–15] In general, their thermodynamic stability was found to be similar or slightly higher than that of the corresponding Sr^{II} complexes. Some Eu^{II} crown ether and azacryptand complexes have also been reported in the literature;[16–18] interestingly they have more positive Eu^{III}/Eu^{II} reduction potentials than the Eu^{III}/Eu^{II} aqua complex which makes them the most redox stable Eu^{II} complexes in aqueous solution found so far.

Among azacrown ethers, the complexation properties of [18]aneN_2O_4-carboxylate derivatives were investigated in detail[19–20] ([18]aneN_2O_4 = 1,4,10,13-tetraoxa-7,16-diaza-cyclooctadecane). Due to the relatively large cavity of the 18-membered macrocycle, its derivatives form especially stable complexes with the divalent and trivalent ions of large ionic radius, and with the rare-earth ions. Moreover, the [18]ane-N_2O_4-dimalonate ($ODDM^{4-}$) shows a large selectivity for Sr^{II} against Ca^{II}.[21] These observations urged us to investigate the thermodynamic and redox stability as well as the water exchange rate of the Eu^{II} complexes of two [18]aneN_2O_4-carboxylate derivatives, namely the 1,4,10,13-tetraoxa-7,16-diaza-cyclooctadecane-7,16-diacetate ($ODDA^{2-}$), and -dimalonate ($ODDM^{4-}$) (chemical structure of the ligands in Scheme 1.). As no X-ray crystal structure is available for either strontium or europium(II) poly(amino carboxylates), attempts have also been made to prepare appropriate crystals for X-ray structural determination of this type of complexes.

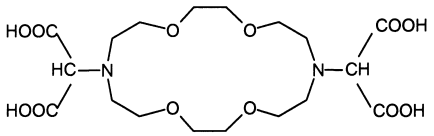

H_4ODDM

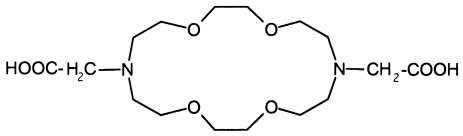

H_2ODDA

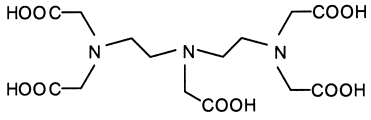

H_5DTPA

Scheme 1. Chemical structure of the ligands.

In the present paper we report thermodynamic stability constants, redox potentials, and the results of proton and oxygen-17 relaxation studies of the $[Eu^{II}(ODDA)(H_2O)]$ and $[Eu^{II}(ODDM)]^{2-}$ complexes. For the first time, we also report the X-ray structure of a Eu^{II} chelate, $[Eu^{II}(DTPA)(H_2O)]^{3-}$, in comparison with the corresponding $[Sr(DTPA)(H_2O)]^{3-}$. The crystal structure of the [Sr(ODDA)] complex is also presented.

Results and Discussion

Crystal structures of $[C(NH_2)_3]_3[Eu^{II}(DTPA)(H_2O)]\cdot 8H_2O$, $[C(NH_2)_3]_3[Sr(DTPA)(H_2O)]\cdot 8H_2O$ and $[Sr(ODDA)]\cdot 8H_2O$: Since so far no solid state X-ray studies have been reported for Eu^{II} chelates, our objective was the structural description of Eu^{II} complexes and their comparison to the analogue complexes formed with Sr^{2+}, which has similar ionic size and charge, but very different electronic configuration. Furthermore, their comparison with the corresponding trivalent lanthanide complexes is also of interest. Solid state X-ray structures are known for numerous lanthanide(III) poly(amino carboxylates)[5] used for biomedical application. In those formed with octadentate ligands, the lanthanide(III) ion is usually nine-coordinate with one water molecule in the inner coordination sphere.

The X-ray structure of $[Eu^{II}(DTPA)(H_2O)]^{3-}$ is shown in Figure 1; the structure of the $[Sr(DTPA)(H_2O)]^{3-}$ analogue is identical (see Supporting Information Figure S1). Selected

  0947-6539/00/0620-3762 $ 17.50+.50/0 *Chem. Eur. J.* **2000**, *6*, No. 20

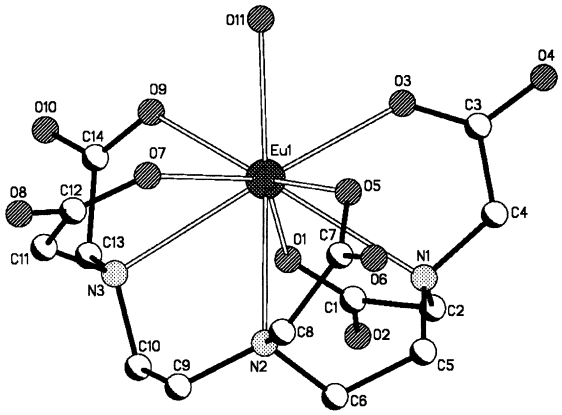

Figure 1. X-ray structure of $[Eu^{II}(DTPA)(H_2O)]^{3-}$.

bond lengths between the coordinating atoms and the metal center as well as selected bond angles are presented in Table 1. (The detailed results can be found in the Supporting Information.)

The coordination number of both divalent metals is nine, with one inner sphere water molecule. Importantly, the bond lengths and angles in both complexes are identical. The coordination polyhedron is close to a regular capped square antiprism, as the two planes formed by O3–O5–O7–O9 and O1–N1–N2–N3 are almost parallel: The angle between the two planes is 3.6 and 3.3° for the Sr^{II} and Eu^{II} compound, respectively.

The crystal structures of $[Sr(DTPA)(H_2O)]^{3-}$ and $[Eu^{II}(DTPA)(H_2O)]^{3-}$ are also similar to that of the $[Gd(DTPA)(H_2O)]^{2-}$ complex, with the exception of the bond lengths. Due to the lower charge and the larger ionic radius of Sr^{2+} and Eu^{2+}, the bond lengths are about 0.15 Å longer than those of the corresponding Gd^{III} complex.[22] For example, the distance between the metal center and the coordinated water oxygen ranges from 2.408 to 2.490 Å for Gd^{III} DTPA-type complexes in general[5] (it is 2.490 Å for $[Gd(DTPA)(H_2O)]^{2-}$),[22] while it is 2.619(4) and 2.622(6) Å in $[Sr(DTPA)(H_2O)]^{3-}$ and $[Eu^{II}(DTPA)(H_2O)]^{3-}$, respectively. These distances agree well with the $Sr-O_{water}$ bond length in $[Sr(H_2O)_{7.3}]^{2+}$ determined by XAFS in solution (2.62 Å).[23] In contrast to the different distances, the average angles between the coordinated water molecule and the carboxylate oxygens are very similar: 73.4° in $[Gd(HDTPA)(H_2O)]^{-}$[24] compared with 76.3(2)° in the $[Eu^{II}(DTPA)(H_2O)]^{3-}$ complex and 76.6(2)° for the Sr complex (bond angles are not reported for the nonprotonated $[Gd(DTPA)(H_2O)]^{2-}$).

Unfortunately, suitable crystals of Eu^{II}(ODDA) could not be obtained. However, the identical structures found for $[Eu^{II}(DTPA)(H_2O)]^{3-}$ and $[Sr(DTPA)(H_2O)]^{3-}$ strongly suggest that all structural data obtained for the Sr^{II} analogue can be applied for Eu^{II}(ODDA) as well. The Sr(ODDA) crystallized as a linear polymer without inner sphere water molecule. In this structure, four oxygens and two nitrogens of the macrocyclic ring and one oxygen of each carboxylate group are bound to the Sr^{2+}, giving eight of the total nine bonds around the metal (Figure 2). The ninth coordination site is occupied by a carboxylate oxygen coming from a neighbor

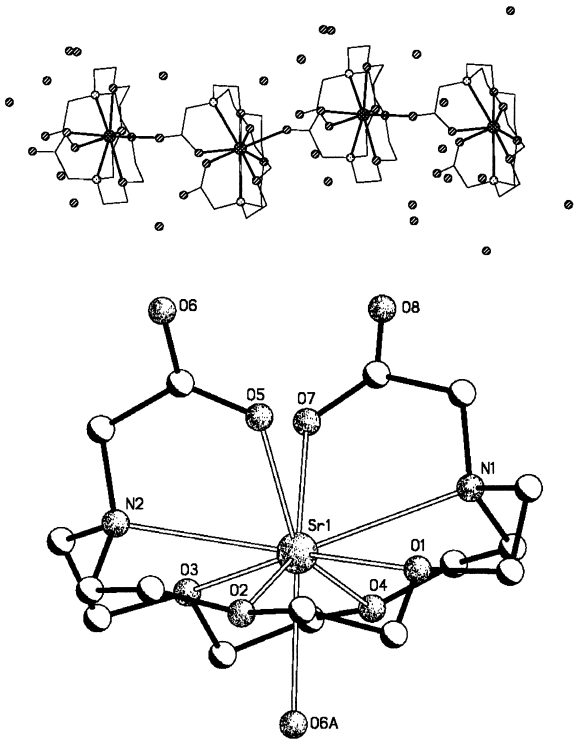

Figure 2. X-ray structure of [Sr(ODDA)].

Table 1. Selected bond lengths [Å] and angles [°] of the complexes obtained from X-ray structures.

	$[Sr(DTPA)(H_2O)]^{3-}$	$[Eu^{II}(DTPA)(H_2O)]^{3-}$	$[Gd(DTPA)(H_2O)]^{2-}$[a]	[Sr(ODDA)]	
M1–O1	2.556(3)	2.568(5)	2.363	Sr1–O1	2.635(4)
M1–O3	2.558(3)	2.569(5)	2.402	Sr1–O2	2.646(4)
M1–O5	2.556(3)	2.569(4)	2.403	Sr1–O3	2.627(4)
M1–O7	2.566(3)	2.562(5)	2.416	Sr1–O4	2.702(4)
M1–O9	2.589(3)	2.600(4)	2.437	Sr1–O5	2.594(4)
M1–O11	2.619(4)	2.622(6)	2.710	Sr1–O6A[c]	2.544(4)
M1–N1	2.910(3)	2.888(6)	2.582	Sr1–O7	2.527(5)
M1–N2	2.784(4)	2.776(5)	2.629	Sr1–N1	2.776(6)
M1–N3	2.769(3)	2.760(5)	2.490	Sr1–N2	2.762(6)
O3–M1–O11	74.6(2)	74.8(3)	68.8[b]	O6A–Sr1–O1[c]	85.4(1)
O5–M1–O11	77.0(1)	76.9(2)	77.2[b]	O6A–Sr1–O2[c]	69.9(1)
O7–M1–O11	73.4(2)	72.7(3)	72.6[b]	O6A–Sr1–O3[c]	76.5(1)
O9–M1–O11	81.3(2)	80.7 (2)	75.1[b]	O6A–Sr1–O4[c]	72.9(1)

[a] Ref. [22]. [b] Bond angles for $[Gd(HDTPA)(H_2O)]^{-}$ from ref. [24]. [c] O6A atom obtained by the following symmetry transformation: $x, -y+\frac{1}{2}, z+\frac{1}{2}$.

ligand. In aqueous solution, this bond breaks up and one water molecule enters the inner coordination sphere, as it is proved by ^{17}O NMR for the analogue Eu^{II} system (see below). Interestingly, in this structure assumed for the aqueous solution, the coordination of the inner sphere water and that of the carboxylates occur on the opposite sides of the molecule. In all poly(amino carboxylate) complexes where structures are known, the inner sphere water coordinates from the carboxylate side of the ligand, thus, constituting a well defined hydrophilic region on this side, in contrast to the hydrophobic region determined by the ligand backbone on the other side of the molecule. This separation of a hydrophobic and hydrophilic side is missing for the Sr(ODDA) and Eu^{II}(ODDA) complexes.

In Sr(ODDA), the metal ion is displaced by 0.641 Å from the plane formed by the four ring oxygens (O1, O2, O3, O4), while the angle between the plane N1–Sr1–N2 and O5–Sr1–O7 is 113.1°. The two carboxylate groups are in *cis*-configuration as referred to the macrocyclic ring, where the angle of O7–Sr1–O5 is 79.3(1)°. Interestingly, for the Cu(ODDA) complex a *trans*-configuration was found.[25] It was explained with the cavity size of the macrocyclic ring which is large enough to accommodate the small Cu^{2+} ion (ionic radius 73 pm). Apparently, the Sr^{2+} (ionic radius 126 pm) is too large to be able to enter the ring cavity. This is also reflected by the longer average bond lengths with the ring oxygens and nitrogens (2.653(4) and 2.769(6) Å, respectively), as compared with that for the carboxylate oxygens (Sr1–O5 = 2.594(4) Å, Sr1–O6A = 2.544(4) Å, Sr1–O7 = 2.527(5)). The Sr1–O5 and Sr1–O6A distances correspond to metal–carboxylate bonds where both oxygens of the carboxylate group are coordinated acting as a bridge between two different metal ions, and consequently these distances are slightly longer than the Sr1–O7 distance. Most of the carboxylate oxygen–metal and nitrogen–metal bond lengths are very close to those obtained for $[Eu^{II}(DTPA)(H_2O)]^{3-}$ and $[Sr(DTPA)(H_2O)]^{3-}$ (Table 1). Furthermore, the average values of the $O_{carboxylate}$–metal ion–O_{water} bond angles in $[Eu^{II}(DTPA)(H_2O)]^{3-}$ and $[Sr(DTPA)(H_2O)]^{3-}$ are also similar to the $O_{macrocycle}$–Sr1–O6A bond angles in Sr(ODDA) (76.2(1)°). However, taking into account the larger bond lengths of the $O_{macrocycle}$–Sr^{2+} in Sr(ODDA), this similarity means that when dissolved in water and the O6A is replaced by a water molecule, the [Sr(ODDA)(H_2O)], and the corresponding [Eu(ODDA)(H_2O)] complexes will be much more open from the water coordination side than the DTPA complexes.

Redox stability of $[Eu^{II}(ODDM)]^{2-}$ and $[Eu^{II}(ODDA)(H_2O)]$: The redox stability of Eu^{II} complexes in aqueous solution is directly described by the redox potential of the $Eu^{III}L/Eu^{II}L$ redox couple; a more negative potential indicates a lower redox stability against oxidation. It is generally assumed that the Eu^{II} ion can oxidize by reacting with both oxygen and water.[10]

As the cyclovoltammetry curves show (Figure 3), the macrocyclic $[Eu^{II}(ODDA)(H_2O)]$ and $[Eu^{II}(ODDM)]^{2-}$ complexes are much more redox stable than $[Eu^{II}(DTPA)(H_2O)]^{3-}$, the redox potentials are $E_{1/2} = -0.92$ and -0.82 V

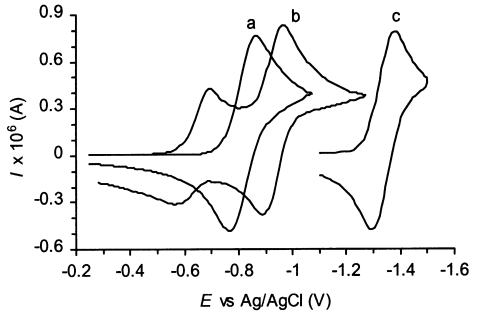

Figure 3. Cyclovoltammograms of a) $Eu^{III/II}$(ODDA), b) $Eu^{III/II}$(ODDM) at 50% metal excess and c) $Eu^{III/II}$(DTPA) solutions.

for $Eu^{III/II}$(ODDM) and $Eu^{III/II}$(ODDA), respectively, compared with $E_{1/2} = -1.35$ V for $Eu^{III/II}$(DTPA).[9] Although the redox potentials of the macrocyclic complexes are still negative, they are much closer to that of $Eu^{III/II}$·aqua. (The signal of the $Eu^{III/II}$·aqua system can also be seen on the cyclovoltammogram of $Eu^{III/II}$(ODDM), as it was recorded at 50% metal excess (Figure 3, curve b), thus the smaller peaks with $E_{1/2} = -0.63$ V correspond to the free $Eu^{III/II}$.)

The redox kinetic behavior of $[Eu^{II}(ODDM)]^{2-}$ and $[Eu^{II}(ODDA)(H_2O)]$ has been studied by UV/Vis spectrometry. The spectrum of $[Eu^{II}(ODDA)(H_2O)]$ shows two maxima at 337 nm ($\varepsilon = 665\,M^{-1}cm^{-1}$) and 262 nm ($\varepsilon = 2013\,M^{-1}cm^{-1}$), while for $[Eu^{II}(ODDM)]^{2-}$ only one peak can be found at 258 nm ($\varepsilon = 2474\,M^{-1}cm^{-1}$) with a shoulder at around 320 nm (see Supporting Information Figures S2a–b). The oxidation of the complexes can be followed by the intensity diminution of the peaks at 262 and 258 nm. The kinetic curves obtained were not first-order and showed a complicated oxidation behavior as it was also observed for $[Eu^{II}(DTPA)(H_2O)]^{3-}$,[9] thus, we could only calculate an approximate value for the half-life time. The redox kinetic stability of the macrocyclic complexes is much higher than that of $[Eu^{II}(DTPA)(H_2O)]^{3-}$: The estimated $t_{1/2}$ is 16 h and 10 d for $[Eu^{II}(ODDM)]^{2-}$ ($c = 1$ mM) and $[Eu^{II}(ODDA)(H_2O)]$ ($c = 5$ mM), respectively, whereas it was only 1 h for $[Eu^{II}(DTPA)(H_2O)]^{3-}$. In all cases the redox stability was found to increase with increasing concentration, for example, a 0.1M, basic $[Eu^{II}(ODDA)(H_2O)]$ solution can be kept under nitrogen without any changes for one month. Such concentration dependence is often observed in the oxidation of strongly reducing agents, and suggests that the oxidation reaction can partly be due to the presence of oxidative trace impurities.

Thermodynamic stability of the complexes: The protonation constants, K_i^H of the ligands $ODDA^{2-}$ and $ODDM^{4-}$, as well as the thermodynamic stability constants, K_{ML} and K_{ML}^H of their Eu^{II} and Sr^{II} complexes are shown in Table 2. For comparison, the table contains also the corresponding constants of the DTPA complexes. The protonation constants determined for $ODDA^{2-}$ and $ODDM^{4-}$ agree well with those previously reported in the literature for similar ionic strength and temperature. The stability constants of the Eu^{II} macrocyclic complexes are more than one order of magnitude higher than those of the Sr analogues, while the protonation constants of the complexes are essentially the same. A similar

0947-6539/00/0620-3764 $ 17.50+.50/0 *Chem. Eur. J.* **2000**, *6*, No. 20

Table 2. Protonation constants of the ligands ($\log K_i^H$), and stabilility and protonation constants ($\log K_{ML}$ and $\log K_H^{ML}$) of the complexes in 0.1M $(CH_3)_4NCl$ at 25 °C.

	$ODDM^{4-}$		$ODDA^{2-}$			$DTPA^{5-}$
	this work	[a]	this work	[b]	[c]	[d]
$\log K_1^H$	8.60 ± 0.02	8.62	8.95 ± 0.02	8.45	8.93	10.59
$\log K_2^H$	8.00 ± 0.01	7.95	7.99 ± 0.02	7.80	8.01	8.65
$\log K_3^H$	3.31 ± 0.02	4.02	2.24 ± 0.03	2.90	2.50	4.28
$\log K_4^H$					2.73	
$\log K_5^H$					2.06	
$\log K_{EuL}$	13.07 ± 0.04		9.85 ± 0.02			10.08
$\log K_{EuL}^H$	4.42 ± 0.02		4.97 ± 0.05			5.45
$\log K_{SrL}$	11.34 ± 0.06		8.66 ± 0.02	8.29		9.68
$\log K_{SrL}^H$	4.56 ± 0.08		4.92 ± 0.12			5.4

[a] Ref. [21] in 0.15M $(CH_3)_4NCl$. [b] Ref. [19]. [c] Ref. [20] in 0.1M $(CH_3)_4NNO_3$. [d] Protonation constants from A. E. Martell, R. M. Smith, *Critical Stability Constants*, *Vol. 1*, Plenum Press, New York, **1974**, p. 281, stability constants from ref. [14].

trend was observed for open-chain poly(amino carboxylate) complexes, such as $DTPA^{5-}$, where the stability of the Eu^{II} complex was identical or slightly higher than that of the Sr complex.[13–14]

The species distribution diagram of Eu^{2+}-$ODDM^{4-}$ (Figure 4a) and Eu^{2+}–$ODDA^{2-}$ (Figure 4b) systems shows that the complexation is complete by pH 7 for $[Eu^{II}(ODDM)]^{2-}$ and pH 7.5 for $[Eu^{II}(ODDA)(H_2O)]$. Similar distribution diagrams were obtained for the Sr complexes except that the protonated complexes form in lower amount (see Supporting Information Figure S3). Compared with $[Eu^{II}(DTPA)(H_2O)]^{3-}$, the macrocyclic complexes have a higher conditional stability due to the lower sum of the ligand protonation constants. This is also reflected in the fact that the $[Eu^{II}(DTPA)(H_2O)]^{3-}$ forms completely only above pH 9.

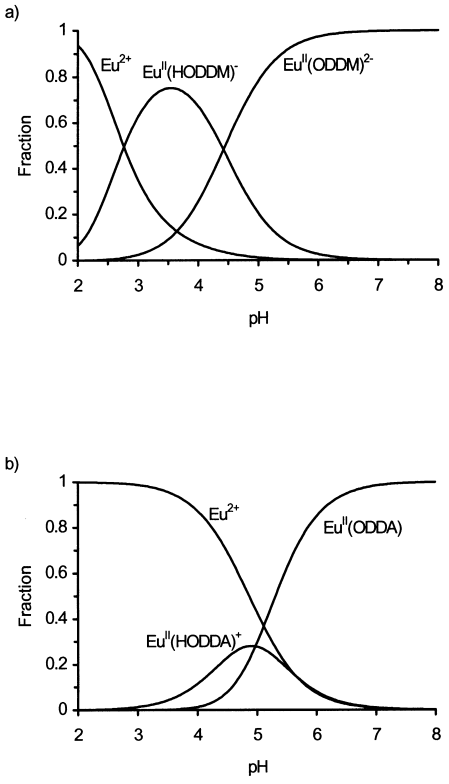

Figure 4. Species distribution diagram of the a) Eu^{2+}–$ODDM^{4-}$ and b) Eu^{2+}–$ODDA^{2-}$ systems.

^{17}O-NMR and NMRD measurements: A variable-temperature oxygen-17 and a variable-temperature and a multiple field proton relaxation study have been performed on $[Eu^{II}(ODDM)]^{2-}$ and $[Eu^{II}(ODDA)(H_2O)]$ to determine the correlation times for water exchange, rotation and electronic relaxation.

For the analysis of both ^{1}H- and ^{17}O-NMR data it is necessary to know the number of inner sphere coordinated water molecules (q). Based on the identical X-ray structures obtained for $[Eu^{II}(DTPA)(H_2O)]^{3-}$ and $[Sr(DTPA)(H_2O)]^{3-}$, the structure of $Eu^{II}(ODDA)$ can also be assumed to be analoguos to that determined for $Sr^{II}ODDA$. This latter does not contain any inner sphere water in solid state, however, the ^{17}O-NMR chemical shifts measured in $[Eu^{II}(ODDA)(H_2O)]$ solutions clearly indicate the presence of inner sphere water. Based on the value of the chemical shifts, or more precisely on the scalar coupling constant, $A/\hbar$, calculated from the shifts we assume $q = 1$ for $[Eu^{II}(ODDA)(H_2O)]$. This constant characterizes the electron delocalization from the ion onto the ligand nucleus, so its value has to be similar for similar complexes. The $A/\hbar$ obtained for $[Eu^{II}(ODDA)(H_2O)]$ is a somewhat higher than that for $[Eu(H_2O)_8]^{2+}$ and $[Eu^{II}(DTPA)(H_2O)]^{3-}$ (Table 3), which could indicate that the average number of inner sphere water molecules in the ODDA complex is more than one due to a hydration equilibrium between differently hydrated species ($q = 1$ and $q = 2$). Such a hydration equilibrium can be influenced by pressure, that is, an increase in pressure will favor the bishydrated species resulting in increased ^{17}O chemical shift values. We have measured the ^{17}O chemical shift of the water signal as a function of pressure up to 165 MPa in a $[Eu^{II}(ODDA)(H_2O)]$, as well as in a $[Sr(ODDA)(H_2O)]$ reference solution. The ^{17}O shifts of the $[Eu^{II}(ODDA)(H_2O)]$ sample referred to the reference solution do not change with pressure within the experimental

Table 3. Parameters obtained from the simultaneous fit of variable-temperature ^{17}O relaxation rates, chemical shifts and ^{1}H NMRD data.

	$[Eu^{II}(H_2O)_8]^{2+}$[a]	$[Eu^{II}(DTPA)(H_2O)]^{3-}$[b]	$[Eu^{II}(ODDA)(H_2O)]$
$k_{ex}^{298}/10^9\ s^{-1}$	4.4	1.3	0.43 ± 0.08
$\Delta H^{\neq}/kJ\ mol^{-1}$	15.7	26.3	22.5 ± 2.6
$\Delta S^{\neq}/J\ mol^{-1}\ K^{-1}$	−7.0	+18.4	-4.0 ± 0.5
$\Delta V^{\neq}/cm^3\ mol^{-1}$	−11.3	+4.5	-3.9 ± 0.1
$(A/\hbar)/10^6\ rad\ s^{-1}$	−3.7	−3.5	-4.3 ± 0.4[c]
τ_R^{298}/ps	16.3	74	58.2 ± 1.6
$E_R/kJ\ mol^{-1}$	21.3	18.9	23.9 ± 0.8
τ_v^{298}/ps	1.0	13.6	14.3 ± 0.7
$E_v/kJ\ mol^{-1}$	12.5	*1*	*1*
$\Delta^2/10^{20}\ s^{-2}$	1.13	1.7	1.01 ± 0.05
$D_{EuL}^{298}/10^{-10}\ m^2\ s^{-1}$	22.9	23	24.3 ± 0.2[d]
$E_{DeuH}/kJ\ mol^{-1}$	20.1	29	25.4 ± 0.7[d]

[a] Ref. [8] simultaneous fit with EPR data. [b] Ref. [9]. [c] Calculated with considering of the outer-sphere contribution obtained from the reduced ^{17}O shift of $[Eu^{II}(ODDM)]^{2-}$. The outer-sphere contribution is 20 ± 7% to the total shift of $[Eu(ODDA)(H_2O)]$. [d] Calculated from the ^{1}H NMRD data of $[Eu^{II}(ODDM)]^{2-}$ and were fixed in the simultaneous fit.

errors, which excludes any hydration equilibrium. Therefore we can conclude that the complex exists as the monohydrated $[Eu^{II}(ODDA)(H_2O)]$ species in aqueous solution.

For $[Eu^{II}(ODDM)]^{2-}$ no solid X-ray data are available. The very small ^{17}O chemical shifts induced by the complex and the identical $1/T_{1r}$ and $1/T_{2r}$ values measured (Figure 5c, 5d, 5e) let us conclude that $[Eu^{II}(ODDM)]^{2-}$ has no inner-sphere water molecule. (The meaning of reduced value here: P_m is considered as the concentration of the complex divided by the molality of the water.) Consequently, $[Eu^{II}(ODDM)]^{2-}$ can be regarded as an outer sphere model for $[Eu^{II}(ODDA)(H_2O)]$. This is rather fortunate because for the two Eu^{II} complexes studied so far by ^{17}O-NMR spectroscopy[8–9] we had to assume that there is no outer sphere contribution to the chemical shifts (there was no slow exchange region where the chemical shifts give indication on the outer sphere contribution), whereas it is well-known that for Gd^{III} complexes it can contribute up to 20% to the overall chemical shift. Therefore, the ^{17}O chemical shift data of $[Eu^{II}(ODDM)]^{2-}$ have been fitted as the outer-sphere contribution to the total shift obtained for $[Eu^{II}(ODDA)(H_2O)]$ [see Appendix Eq. (5)]. This outer-sphere contribution to the ^{17}O chemical shift was found to be $20 \pm 7\%$ to the total shift of $[Eu^{II}(ODDA)(H_2O)]$. Similarly, the $[Eu^{II}(ODDM)]^{2-}$ was used as an outer-sphere model for the proton relaxivities as well.

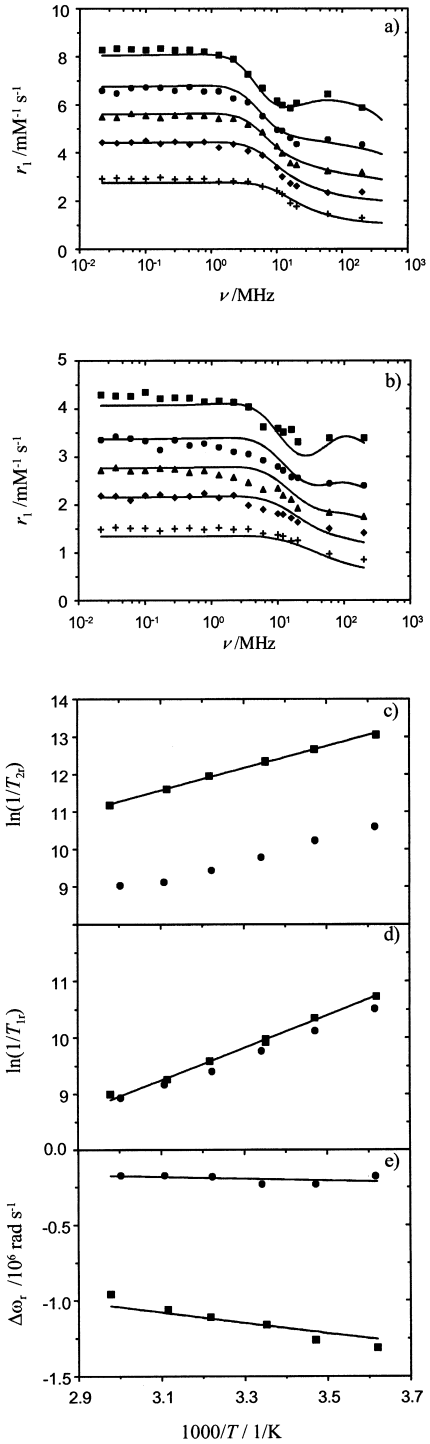

Figure 5. ^1H-NMRD profiles of a) $[Eu^{II}(ODDA)(H_2O)]$, b) $[Eu^{II}(ODDM)]^{2-}$ solutions at 5 °C (■), 15 °C (●), 25 °C (▲), 37 °C (◆) and 60 °C (+). c) Reduced transverse and d) longitudinal ^{17}O relaxation rates and e) chemical shifts at $B = 9.4$ T for $[Eu^{II}(ODDA)(H_2O)]$ (■) and for $[Eu^{II}(ODDM)]^{2-}$ (●).

The proton relaxivities (r_1), the reduced ^{17}O relaxation rates ($1/T_{1r}$ and $1/T_{2r}$) and chemical shifts ($\Delta\omega_r$) of $[Eu^{II}(ODDA)(H_2O)]$, together with the $\Delta\omega_r$ values of $[Eu^{II}(ODDM)]^{2-}$, were fitted simultaneously to the theory (for the equations see Appendix) that has already been successfully applied for several Gd^{III} complexes as well as for Eu^{II} aqua and for $[Eu^{II}(DTPA)(H_2O)]^{3-}$.[26, 8, 9] The experimental data and fits are presented in Figure 5 and the parameters obtained are given in Table 3. The diffusion coefficient, D^{298}_{EuH}, was fixed to the value obtained for $[Eu^{II}(ODDM)]^{2-}$ in a separate fit of the proton relaxivities to the outer sphere relaxation theory [see Appendix for Eqs. (17), (18), and (19)]. For the Eu–O distance, r_{EuO}, we used the value determined for $[Eu^{II}(DTPA)(H_2O)]^{3-}$ by solid state X-ray (2.62 Å) and for the Eu–H distance we used $r_{EuH} = 3.22$ Å.

The pressure dependence of the reduced transverse relaxation rates, $1/T_{2r}$, was measured for $[Eu^{II}(ODDA)(H_2O)]$ at 298 K and 9.4 T. At this temperature and magnetic field $1/T_{2r}$ is in the fast exchange limit. The hyperfine coupling constant, $A/\hbar$, and τ_v was assumed pressure independent.[27] (When a pressure dependence equivalent to activation volumes between -4 and $+4$ cm^3 mol^{-1} was ascribed to τ_v, the change in the fitted parameters was less than 5%.) Thus, the measured $1/T_{2r}$ values are directly proportional to the exchange rate, k_{ex}. The data points and the least square fit are shown in Figure 6, and the fitted parameters are $(k_{ex})^{298}_0 = (4.46 \pm 0.02) \times 10^8$ s^{-1} and $\Delta V^{\neq} = -3.9 \pm 0.1$ cm^3 mol^{-1}.

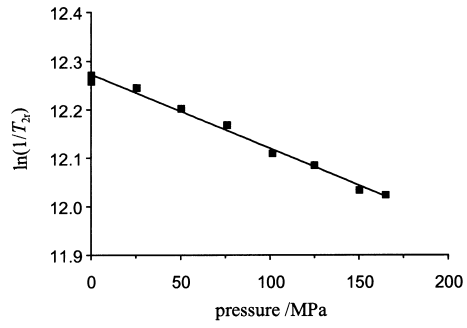

Figure 6. Pressure dependence of the reduced transverse ^{17}O relaxation rates at $B = 9.4$ T and 25 °C for $[Eu^{II}(ODDA)(H_2O)]$.

0947-6539/00/0620-3766 $ 17.50+.50/0 *Chem. Eur. J.* **2000**, *6*, No. 20

Water exchange on [Eu^{II}(ODDA)(H$_2$O)]: The water exchange rate of the complex is determined from the transverse ^{17}O relaxation rates ($1/T_{2r}$). In the whole temperature range studied, the system is in the fast exchange region (see Figure 5c), thus, the $1/T_{2r}$ values are given by the relaxation rate of the coordinated water molecule ($1/T_{2m}$), itself determined by the water residence time ($\tau_m = 1/k_{ex}$), the longitudinal electronic relaxation rate ($1/T_{1e}$), and the nuclear hyperfine coupling constant ($A/\hbar$) [see Appendix for Eq. (7)].

The water exchange rate, k_{ex}^{298}, is ten times lower on [Eu^{II}(ODDA)(H$_2$O)] than on [Eu(H$_2$O)$_8$]$^{2+}$ and about one third of that on [Eu^{II}(DTPA)(H$_2$O)]$^{3-}$ (Table 3).[5, 9] The negative activation volume indicates associatively activated interchange ($\mathbf{I_a}$) mechanism,[28] which is also supported by the negative activation entropy. For [Eu^{II}(DTPA)(H$_2$O)]$^{3-}$, the water exchange mechanism was found to be dissociatively activated with an eight-coordinate transition state.[9] The difference in the water exchange mechanism on the [Eu^{II}(ODDA)(H$_2$O)] and [Eu^{II}(DTPA)(H$_2$O)]$^{3-}$ complexes is not unexpected if the structure of the two complexes is taken into account (we assume that [Eu^{II}(ODDA)(H$_2$O)] is isostructural with the Sr analogue where the crystal structure is known). The distances between the metal and the coordinating atoms as well as the bond angles show that the water coordinating site is much more open in the ODDA than in the DTPA complex. As a consequence, the [Eu^{II}(ODDA)(H$_2$O)] can accommodate a second water molecule in the inner sphere without the preceding departure of the leaving water molecule, whereas in [Eu^{II}(DTPA)(H$_2$O)]$^{3-}$ the inner sphere water has to leave first in order to provide enough room for the entering molecule. The difference in the exchange rates, though not enormous, can also be the consequence of the different mechanisms. However, in order to be able to draw general trends for water exchange rates on Eu^{II} complexes further systems have to be measured.

Rotation: The rotation correlation time, τ_R, of the complex is calculated from the longitudinal water ^{1}H- and ^{17}O relaxation rates. The simultaneous fit of ^{1}H- and ^{17}O-NMR data gave $\tau_R^{298} = 58$ ps for [Eu^{II}(ODDA)(H$_2$O)] which is about 25% lower than that obtained for [Eu^{II}(DTPA)(H$_2$O)]$^{3-}$. The faster rotation can be explained by the fact that [Eu^{II}(ODDA)(H$_2$O)] is a neutral complex, thus, the whole tumbling entity is smaller than for example, in the case of the triple-charged DTPA-chelate.

Electronic relaxation: The electronic relaxation parameters (the trace of the square of transient zero-field-splitting, Δ^2, and the correlation time for the modulation of ZFS, τ_v) have been obtained from the simultaneous fit of ^{1}H NMRD and ^{17}O relaxation data for [Eu^{II}(ODDA)(H$_2$O)] and from the separate fit of ^{1}H NMRD data for [Eu^{II}(ODDM)]$^{2-}$. For [Eu^{II}(ODDA)(H$_2$O)], they are mainly determined by the NMRD data, as electronic relaxation contributes less than 6% to the transverse ^{17}O relaxation rates at 9.4 T. The values obtained are $\Delta^2 = (1.01 \pm 0.05) \times 10^{20}\ s^{-2}$ and $(1.94 \pm 0.27) \times 10^{20}\ s^{-2}$ for [Eu^{II}(ODDA)(H$_2$O)] and [Eu^{II}(ODDM)]$^{2-}$, respectively, compared with $\Delta^2 = 1.7 \times 10^{20}\ s^{-2}$ for [Eu^{II}(DTPA)(H$_2$O)]$^{3-}$.[9] As τ_v is quite similar for the three complexes (14.3 ± 0.7 ps, 11.6 ± 1.2, and 13.6 ps for [Eu^{II}(ODDA)(H$_2$O)], [Eu^{II}(ODDM)]$^{2-}$, and [Eu^{II}(DTPA)(H$_2$O)]$^{3-}$, respectively) we can predict a narrower EPR band for [Eu^{II}(ODDA)(H$_2$O)] and a somewhat broader one for [Eu^{II}(ODDM)]$^{2-}$ than for [Eu^{II}(DTPA)(H$_2$O)]$^{3-}$. A multiple field EPR study is in progress to investigate electronic relaxation of Eu^{II} complexes.

Proton relaxivity: The measured longitudinal water proton relaxation rates, r_1, of [Eu^{II}(ODDA)(H$_2$O)] and [Eu^{II}(ODDM)]$^{2-}$ solutions are presented in Figure 5a and 5b. (The values are normalized for 1 mM Eu^{II} concentration.) Considering the large magnetic field covered in this study (5×10^{-4} to 0.47 T) the fit of the data is quite satisfying. The relaxivity of [Eu^{II}(ODDA)(H$_2$O)] at 20 MHz and 25 °C is 3.49 mM^{-1} s^{-1} which is similar to that of [Eu^{II}(DTPA)(H$_2$O)]$^{3-}$ under the same conditions (3.57 mM^{-1} s^{-1}).[9] Although the water exchange rate is in the optimal range to obtain maximum relaxivities, the fast rotation of the small molecular weight complexes avoids attaining higher values. If attached to a slowly rotating macromolecule, these Eu^{II} agents could have about 10 times higher proton relaxivities.

Conclusion

The first solid X-ray crystal structure of a Eu^{II} chelate, [Eu^{II}(DTPA)(H$_2$O)]$^{3-}$, has been found identical with that of the Sr analogue. In solid state the macrocyclic [Sr^{II}(ODDA)] complex forms linear polymer chains with carboxylate bridges and has no inner-sphere water. The crystal structure is most likely to be the same for the Eu^{II} analogue as well. In solution the bridging carboxylate group is replaced by a water molecule, as determined by ^{17}O chemical shifts for the [Eu^{II}(ODDA)(H$_2$O)]. Interestingly, this is the only lanthanide chelate reported so far where the inner sphere water molecule and the carboxylates coordinate to the metal from the opposite sides of the macrocyclic plane. Both the thermodynamic and redox stabilities (several weeks) of the macrocyclic [Eu^{II}(ODDA)(H$_2$O)] and [Eu^{II}(ODDM)]$^{2-}$ complexes are higher than those of [Eu^{II}(DTPA)(H$_2$O)]$^{3-}$. Both the higher thermodynamic stability and the stabilization of the lower oxidation state in aqueous solution can be important in biomedical applications of Eu$^{II/III}$ systems such as redox responsive MRI probes. Certainly, beside the thermodynamic and oxidative stability of the complex, kinetic inertness is also of importance for in vivo applications. In a biological environment, due to the competition of other endogenously available metal ions, the kinetic stability of the complex may not be sufficient. However, at physiological pH the proton catalyzed pathway for the dissociation of the complex is not significant.

As the [Eu^{II}(ODDM)]$^{2-}$ has no inner sphere water molecule, it was used as an outer sphere model in the analysis of both ^{17}O NMR and NMRD data for [Eu^{II}(ODDA)(H$_2$O)]. Contrary to [Eu^{II}(DTPA)(H$_2$O)]$^{3-}$, the mechanism of the water exchange is associatively activated for [Eu^{II}(ODDA)(H$_2$O)], which is the consequence of the more open water binding site of the metal ion. The water exchange rate, as

obtained from a simultaneous fit of ^{17}O-NMR and ^{1}H-NMRD data, could be optimal to reach high proton relaxivities. The fast tumbling of the complex prevents attaining higher relaxivity values, however, this can be circumvented by attaching the Eu^{II} chelate to slowly rotating macromolecules.

Experimental Section

H_2ODDA was purchased from Fluka, Na_4ODDM was kindly provided by Prof. Ernö Brücher, (Lajos Kossuth University, Debrecen, Hungary) and used without further purification. The concentration of ligand solutions was determined from the pH potentiometric titration curves obtained in the absence and presence of an excess of $CaCl_2$. The manipulations with ODDM were done at pH > 3 to avoid decarboxylation of the malonate groups in acidic solution.[21] For the preparation of $Eu(O_3SCF_3)_3$, $EuCl_3$, and $SrCl_2$ solutions, we used the salts of the highest analytical grade (Fluka and Alfa Aesar). The concentration of the solutions was determined by complexometric titrations with standardized $Na_2(H_2EDTA)$, using xylenol orange or methylthymol blue indicator. The solutions of the Eu^{II} complexes were prepared by reducing the corresponding Eu^{III} solutions with controlled coulometry in a home built electrolysis cell using an EG&G 263A galvanostate/potentiostate.[9] The reduction potential used was 0.4–0.5 V lower than the $E_{1/2}$ calculated from the cyclovoltammogram of the EuL solution. The solutions of the Eu^{III} complexes were prepared by mixing equimolar quantities of the ligand and the metal and setting the appropriate pH. The cyclovoltammetry curves were recorded on the same EG&G 263A galvanostat/potentiostat apparatus with a standard cell in EuL solution ($c_{EuL} = 0.001$M and 0.1M $NaNO_3$ as supporting electrolyte) using a Pt microelectrode, Ag/AgCl in 3M NaCl reference electrode at 50 mV s^{-1} scan rate. The concentration of the Eu^{II} samples prepared by electrolysis was always determined by a Zimmermann–Reinhardt redox titration using a ten-fold $Fe_2(SO_4)_3$ excess in H_2SO_4/H_3PO_4 solution (4M), then the Fe^{II} formed, corresponding to the amount of Eu^{II}, was titrated with a $K_2Cr_2O_7$ solution. The poly(amino carboxylate) ligands showed no interference with the $K_2Cr_2O_7$ solution. The redox potential of the titrated solution was monitored with a combined Pt redox electrode (reference electrode part 3M KCl Ag/AgCl, Metrohm) connected to a Metrohm 692 pH/ion-meter. The concentration determined in this way corresponded well, within the limit of the precision of the titration, to the Eu quantity weighed in. All manipulations with Eu^{II} samples were done under nitrogen atmosphere with rigorous exclusion of oxygen.

X-ray measurements: To prepare $[C(NH_2)_3]_3[Sr(DTPA)(H_2O)]\cdot 8H_2O$ crystals, H_5DTPA (7.88 g, 20 mmol) was added to a slurry solution of $SrCO_3$ (2.95 g, 20 mmol) in water (30 mL). When the production of CO_2 has finished, $[C(NH_2)_3]_2CO_3$ was added (3.60g, 20 mmol). The pH was adjusted to 10 by NaOH. By addition of acetone a white powder was precipitated in the solution. The received powder was filtered and than redissolved in small amounts of water. Acetone was added until the solution became opalescent. After a few days of storage in refrigerator, small colorless plates were obtained and used for X-ray structural determination.

To obtain $[C(NH_2)_3]_3[Eu^{II}(DTPA)(H_2O)]\cdot 8H_2O$ crystals, $[C(NH_2)_3]_2[Eu^{III}(DTPA)]$ (227 mg, 0.33 mmol) prepared from $EuCO_3$, was dissolved in water (2 mL). After complete electrochemical reduction at pH 9, the solution was filled into a Schlenk tube, closed under N_2 and acetone was added until the solution became opalescent. After keeping the sample in the refrigerator for few days we obtained yellow crystalline plates.

For the preparation of $[Sr(ODDA)]\cdot 8H_2O$ crystals, H_2ODDA (100 mg, 0.27 mmol) and $SrCO_3$ (40 mg) were dissolved in water (0.5 mL). When CO_2 production has finished, the solution (pH 8) was filtrated and the clear filtrate was treated with acetone in the same way as for the DTPA samples.

Suitable crystals were mounted in glass capillaries and measured by the following technique. Data collection for $[C(NH_2)_3]_3[Sr(DTPA)(H_2O)]\cdot 8H_2O$ and $[Sr(ODDA)]\cdot 8H_2O$ was performed on a mar345 imaging plate detector system and data reduction was carried out with marHKL release 1.9.1.[29] Diffraction data for $[C(NH_2)_3]_3[Eu^{II}(DTPA)(H_2O)]\cdot 8H_2O$ were collected on a Rigaku Mercury CCD and reduced with Crystal Clear 1.2.0[30] and teXsan for Windows 1.0.5.[31] Data for $[C(NH_2)_3]_3[Eu^{II}(DTPA)(H_2O)]\cdot 8H_2O$ were then corrected for absorption (REQAB4, release 1.1)[31]. Structure solution for all compounds was performed with ab initio direct methods.[32] All structures were refined using the full-matrix least-squares on F^2 with all non-H atoms anisotropically defined. H atoms were placed in calculated positions using the "riding model" (except the ones belonging to water molecules which were not included in the model) with $U_{iso} = a \times U_{eq}(X)$ (where a is 1.5 for methyl hydrogen atoms and 1.2 for others, while X is the parent atom). Some water molecules in the complexes $[C(NH_2)_3]_3[Sr(DTPA)(H_2O)]\cdot 8H_2O$ and $[Sr(ODDA)]\cdot 8H_2O$ were found to be affected by disorder and split into two different sites. Space group determination, structure solution, refinement, molecular graphics, and geometrical calculation have been carried out on all structures with the SHELXTL software package, release 5.1.[33] Crystal data and structure refinement details are presented in Table 4, and the final atomic coordinates, thermal, and geometrical parameters and hydrogen coordinates are listed in the Supporting Information.

UV/Vis measurements: UV/Vis spectra of the complexes were recorded on a Perkin–Elmer Lambda 5 spectrophotometer. The solutions containing Eu^{II} were filled under nitrogen into special cuvettes suitable for use in anaerobic conditions.

Equilibrium studies: The ligand protonation constants and complex stability constants were determined by pH potentiometry at a constant ionic strength (0.1M $(CH_3)_4NCl$). The titrations were carried out in a thermostated vessel (25 ± 0.2 °C) using $(CH_3)_4NOH$ as titrant solution dosed with a Metrohm Dosimat 665 automate burette and a combined glass electrode (C14/02-SC, reference electrode part Ag/AgCl in 3M KCl, Moeller Scientific Glass Instruments, Switzerland) connected to a Metrohm 692 pH/ion-meter. The titrated solution (3–4 mL) was stirred with a magnetic stirrer and bubbled with a constant N_2 flow to avoid any effects from O_2 and CO_2. Protonation and stability constants were determined in 0.001–0.002M solutions from 3–4 parallel titrations, each curve containing 40–50 volume/pH data pairs in the pH range 2–10 for ODDA and 3–10 for ODDM. To obtain the stability constants of the Eu^{II} complexes, freshly reduced $EuCl_2$ solution was added to the beforehand deoxygenated sample solution and was titrated immediately. The hydrogen ion concentration was calculated from the measured pH values as suggested by Irving, where a correction term is used, obtained as the difference between the measured and calculated pH values in a titration of HCl (0.01M) with standardized $(CH_3)_4NOH$.[34]

^{17}O NMR measurements: For the variable-temperature studies, the $[Eu^{II}(ODDA)(H_2O)]$ ($c = 0.1107$ mol kg^{-1}, pH 8.4) and the $[Eu^{II}(ODDM)]^{2-}$ solutions ($c = 0.0968$ mol kg^{-1}, pH 8.6) were filled with a syringe into glass spheres which were fitted into 10 mm NMR tubes. The NMR tubes containing the spheres had been previously closed with a septum in a glove box under nitrogen. Glass spheres are used in order to eliminate susceptibility effects.[35] The relaxation rates and chemical shifts were measured with regard to a NaOH solution (pH 9) as external reference. To improve sensitivity in ^{17}O NMR, ^{17}O-enriched water (10% $H_2{}^{17}O$, Yeda (Israel)) was added to the solutions to yield in 2% ^{17}O enrichment. The ^{17}O NMR measurements were performed on a Bruker AM-400 spectrometer at 9.4 T, 54.2 MHz. Bulk water longitudinal relaxation rates, $1/T_1$, were obtained by the inversion recovery method,[36] and transverse relaxation rates, $1/T_2$, by the Carr–Purcell–Meiboom–Gill spin echo technique.[37]

Variable-pressure NMR spectra were recorded up to a pressure of 165 MPa on a Bruker AMX-400 spectrometer equipped with a home-made high pressure probe.[38]

NMRD: The $1/T_1$ nuclear magnetic relaxation dispersion (NMRD) profiles of the solvent protons at 5, 15, 25, 37 and 60 °C were obtained in 0.01–0.02M Eu^{II}L solutions on a Spinmaster FFC fast field cycling NMR relaxometer (Stelar), covering a continuum of magnetic fields from 5×10^{-4} to 0.47 T (corresponding to a proton Larmor frequency range 0.022–20 MHz). Higher frequency measurements were performed on a 60 MHz electromagnet, connected to an AC-200 console and on a Bruker AC-200 spectrometer.

Data analysis: The thermodynamic equilibrium constants were calculated by the program PSEQUAD.[39] The ligand protonation constants (K_i^H) the complex stability and protonation constants (K_{ML} and K_{ML}^H) are defined as $K_i^H = [H_iL]/[H_{i-1}L][H^+]$, $K_{ML} = [ML]/[L][M^{2+}]$ and $K_{ML}^H = [HML]/[ML][H^+]$. The simultaneous least-squares fit of ^{17}O-NMR and NMRD

0947-6539/00/0620-3768 $ 17.50+.50/0 Chem. Eur. J. 2000, 6, No. 20

Table 4. Crystal data and structure refinement.

	$[C(NH_2)_3]_3[Sr(DTPA)(H_2O)]\cdot 8H_2O$	$[C(NH_2)_3]_3[Eu^{II}(DTPA)(H_2O)]\cdot 8H_2O$	$[Sr(ODDA)]\cdot 8H_2O$
formula	$C_{17}H_{54}N_{12}O_{19}Sr$	$C_{17}H_{54}N_{12}O_{19}Eu$	$C_{16}H_{44}N_2O_{16}Sr$
M_r	818.34	882.68	608.15
temperature [K]	143(2)	143(2)	143(2)
wavelength	$Mo_{K\alpha}$	$Mo_{K\alpha}$	$Mo_{K\alpha}$
crystal system	Triclinic	Triclinic	Monoclinic
space group	$P1$	$P1$	$P2_1/c$
unit cell dimensions [Å, °]	$a=10.641(2)$ $\alpha=94.21(2)$	$a=10.4575(9)$ $\alpha=94.3575(13)$	$a=10.256(2)$ $\alpha=90$
	$b=10.740(2)$ $\beta=102.18(2)$	$b=10.7425(7)$ $\beta=101.9872(15)$	$b=20.057(4)$ $\beta=109.05(3)$
	$c=17.844(4)$ $\gamma=110.975(10)$	$c=17.836(2)$ $\gamma=110.5455(17)$	$c=13.619(3)$ $\gamma=90$
volume [Å^3]	1836.4(6)	1810.9(3)	2648.1(9)
Z	2	2	4
density (calculated) [g cm^{-3}]	1.480	1.619	1.525
absorption coefficient [mm^{-1}]	1.555	1.820	2.110
$F(000)$	860	910	1280
crystal size [mm^3]	$0.34\times0.20\times0.15$	$0.24\times0.17\times0.10$	$0.35\times0.10\times0.05$
θ range for data collection [°]	1.18 to 25.02	1.18 to 26.38	1.88 to 24.40
index ranges	$-11\le h\le 11$, $-12\le k\le 12$,	$-12\le h\le 9$, $-10\le k\le 11$,	$-11\le h\le 11$, $-21\le k\le 23$,
	$-21\le l\le 21$	$-17\le l\le 21$	$-14\le l\le 14$
reflections collected	11210	8623	12536
independent reflections	5865 [$R_{int}=0.0309$]	4287 [$R_{int}=0.0172$]	3930 [$R_{int}=0.0816$]
refinement method	full-matrix least-squares on F^2	full-matrix least-squares on F^2	full-matrix least-squares on F^2
data/restraints/parameters	5865/0/483	4287/0/482	3930/0/317
final R indices [$I>2\sigma(I)$][a]	$R1=0.0592$, $wR2=0.1639$	$R1=0.0389$, $wR2=0.0929$	$R1=0.0614$, $wR2=0.1547$
R indices (all data)[a]	$R1=0.0619$, $wR2=0.1676$	$R1=0.0420$, $wR2=0.0967$	$R1=0.0925$, $wR2=0.1683$
GoF[b]	1.075	1.113	0.985
extinction coefficient	0.148(7)	–	0.0010(6)
largest diff. peak and hole [e Å^{-3}]	0.879 and −1.106	2.257 and −0.619	1.254 and −1.421

[a] $R=\Sigma||F_o|-|F_c||/\Sigma|F_o|$, $wR2=\{\Sigma[w(F_o^2-F_c^2)^2]/\Sigma[w(F_o^2)^2]\}^{1/2}$. [b] $GoF=\{\Sigma[w(F_o^2-F_c^2)^2]/(n-p)\}^{1/2}$, where n is the number of data and p is the number of parameters refined.

data was performed with the program Scientist for Windows by Micromath, version 2.0. The reported errors correspond to one standard deviation obtained by the statistical analysis.

Crystallographic data (excluding structure factors) for the structures reported in this paper have been deposited with the Cambridge Crystallographic Data Centre as supplementary publication no. CCDC-141713–CCDC-141715. Copies of the data can be obtained free of charge on application to CCDC, 12 Union Road, Cambridge CB21EZ, UK (fax: (+44) 1223-336-033; e-mail: deposit@ccdc.cam.ac.uk).

Appendix

Oxygen-17 NMR: From the measured ^{17}O NMR relaxation rates and angular frequencies of the paramagnetic solutions, $1/T_1$, $1/T_2$, and ω, and of the water reference, $1/T_{1A}$, $1/T_{2A}$, and ω_A, the reduced relaxation rates and chemical shift, $1/T_{1r}$, $1/T_{2r}$, and ω_r can be calculated, which may be written as in Equations (1)–(3), where P_m is the molar fraction of bound water, $1/T_{1m}$, $1/T_{2m}$ are the relaxation rates of the bound water and $\Delta\omega_m$ is the chemical shift difference between bound and bulk water.

$$\frac{1}{T_{1r}}=\frac{1}{P_m}\left[\frac{1}{T_1}-\frac{1}{T_{1A}}\right]=\frac{1}{T_{1m}+\tau_m} \tag{1}$$

$$\frac{1}{T_{2r}}=\frac{1}{P_m}\left[\frac{1}{T_2}-\frac{1}{T_{2A}}\right]=\frac{1\ T_{2m}^{-2}+\tau_m^{-1}T_{2m}^{-1}+\Delta\omega_m^2}{\tau_m\left(\tau_m^{-1}+T_{2m}^{-1}\right)^2+\Delta\omega_m^2} \tag{2}$$

$$\Delta\omega_r=\frac{1}{P_m}\omega-\omega_A)=\frac{\Delta\omega_m}{\left(1+\tau_m T_{2m}^{-1}\right)^2+\tau_m^2\Delta\omega_m^2}+\Delta\omega_{os} \tag{3}$$

$\Delta\omega_m$ is determined by the hyperfine or scalar coupling constant, $A/\hbar$, according to Equation (4), where B represents the magnetic field, S is the electron spin and g_L is the isotropic Landé g factor.

$$\Delta\omega_m=\frac{g_L\mu_B S(S+1)B}{3K_BT}\frac{A}{\hbar} \tag{4}$$

The outer-sphere contribution to the chemical shift is assumed to be linearly related to $\Delta\omega_m$ by a constant C_{os} [Eq. (5)].

$$\Delta\omega_{os}=C_{os}\Delta\omega_m \tag{5}$$

The ^{17}O longitudinal relaxation rates are given by Equation (6), where γ_S is the electron and γ_I is the nuclear gyromagnetic ratio ($\gamma_S=1.76\times10^{11}$ rad s^{-1}T^{-1}, $\gamma_I=-3.626\times10^7$ rad s^{-1}T^{-1}), r is the effective distance between the electron charge and the ^{17}O nucleus, I is the nuclear spin (5/2 for ^{17}O), χ is the quadrupolar coupling constant and η is an asymmetry parameter.

$$\frac{1}{T_{1m}}\left[\frac{1}{15}\left(\frac{\mu_0}{4\pi}\right)^2\frac{\hbar^2\gamma_I^2\gamma_S^2}{r_{EuO}^6}S(S+1)\right]\times\left[6\tau_{d1}+14\frac{\tau_{d2}}{1+\omega_s^2\tau_{d2}^2}\right]+\frac{3\pi^2}{10}\frac{2I+3}{I^2(2I-1)}\chi^2(1+\eta^2/3)\tau_R \tag{6}$$

In the transverse relaxation the scalar contribution, $1/T_{2sc}$, is the most important one [Eq. (7)]. In Equation (7) $1/\tau_{s1}$ is the sum of the exchange rate constant and the electron spin relaxation rate.

$$\frac{1}{T_{2m}}\cong\frac{1}{T_{2sc}}=\frac{S(S+1)}{3}\left(\frac{A}{\hbar}\right)^2\tau_{s1}\frac{1}{\tau_{s1}}=\frac{1}{\tau_m}+\frac{1}{T_{1e}} \tag{7}$$

The binding time (or exchange rate, k_{ex}) of water molecules in the inner sphere is assumed to obey the Eyring Equation [Eq. (8)], where $\Delta S^{\ddagger}$ and $\Delta H^{\ddagger}$ are the entropy and enthalpy of activation for the exchange process, and k_{ex}^{298} is the exchange rate at 298.15 K.

$$\frac{1}{\tau_m}=k_{ex}=\frac{k_BT}{h}\exp\left\{\frac{\Delta S^{\ddagger}}{R}-\frac{\Delta H^{\ddagger}}{RT}\right\}=k_{ex}^{298}T\ 298.15\exp\left\{\frac{\Delta H^{\ddagger}}{R}\left(\frac{1}{298.15}-\frac{1}{T}\right)\right\} \tag{8}$$

The electron spin relaxation rates, $1/T_{1e}$ and $1/T_{2e}$ for metal ions in solution with $S>1/2$ are mainly governed by a transient zero-field-splitting mechanism (ZFS). The ZFS terms can be expressed by Equations (9), (10), and

(11),[40–41] where Δ^2 is the trace of the square of the transient zero-field-splitting tensor, τ_v is the correlation time for the modulation of the ZFS with the activation energy E_v, and ω_s is the Larmor frequency of the electron spin.

$$\left(\frac{1}{T_{1e}}\right)^{ZFS} = \frac{1}{25}\Delta^2\tau_v\{4S(S+1)-3\}\left(\frac{1}{1+\omega_S^2\tau_v^2}+\frac{4}{1+4\omega_S^2\tau_v^2}\right) \quad (9)$$

$$\left(\frac{1}{T_{2e}}\right)^{ZFS} = \Delta^2\tau_v\left[\frac{5.26}{1+0.372\omega_S^2\tau_v^2}+\frac{7.18}{1+1.24\omega_S\tau_v}\right] \quad (10)$$

$$\tau_v = \tau_v^{298}\exp\left\{\frac{E_v}{R}\left(\frac{1}{T}-\frac{1}{298.15}\right)\right\} \quad (11)$$

The pressure dependence of $\ln(k_{ex})$ is linear [Eq. (12)], where $\Delta V^{\neq}$ is the activation volume and $(k_{ex})_0^T$ is the water exchange rate at zero pressure and temperature T.

$$\frac{1}{\tau_m} = k_{ex} = (k_{ex})_0^T\exp\left\{-\frac{\Delta V^{\neq}}{RT}\right\}P \quad (12)$$

NMRD: The measured proton relaxivities (normalized to 1 mM Eu^{2+} concentration) contain both inner sphere and outer sphere contributions [Eq. (13)].

$$r_1 = r_{1is} + r_{1os} \quad (13)$$

The inner sphere term is given by Equation (14), where q is the number of inner sphere water molecules.

$$r_{1is} = \frac{1}{1000}\times\frac{q}{55.55}\times\frac{1}{T_{1m}^H+\tau_m} \quad (14)$$

The longitudinal relaxation rate of inner sphere protons, $1/T_{1m}^H$ can be expressed as in Equation (15).

$$\frac{1}{T^H_{1m}} = \frac{2}{15}(\mu_o 4\pi)^2\frac{\hbar^2\gamma_S^2\gamma_I^2}{r_{EuH}^6}S(S+1)\left[\frac{3\tau_{d1}}{1+\omega_I^2\tau_{d1}^2}+\frac{7\tau_{d2}}{1+\omega_S^2\tau_{d2}^2}\right] \quad (15)$$

In Equation (15) r_{EuH} is the effective distance between the Eu^{II} electron spin and the water protons, ω_I is the proton resonance frequency, and τ_{di} is given by Equation 16.

$$\frac{1}{\tau_{di}} = \frac{1}{\tau_m}+\frac{1}{\tau_R}+\frac{1}{T_{ie}}: i = 1, 2 \quad (16)$$

The outer-sphere contribution can be described by Equation (17) and (18), where N_A is the Avogadro constant, and J_{os} is a spectral density function.

$$r_{los} = \frac{32N_A\pi}{405}\left(\frac{\mu_0}{4\pi}\right)^2\hbar^2\gamma_S^2\gamma_I^2 a_{EuH}D_{EuH}S(S+1)[3J_{os}(\omega_I,T_{1e})+7J_{os}(\omega_S,T_{2e})] \quad (17)$$

$$J_{os}(\omega,T_{je}) = R_e\left[\frac{1+1/4\left(i\omega\tau_{EuH}+\frac{\tau_{EuH}}{T_{je}}\right)^{1/2}}{1+\left(i\omega\tau_{EuH}+\frac{\tau_{EuH}}{T_{je}}\right)^{1/2}+4/9\left(i\omega\tau_{EuH}+\frac{\tau_{EuH}}{T_{je}}\right)+1/9\left(i\omega\tau_{EuH}+\frac{\tau_{EuH}}{T_{je}}\right)^{3/2}}\right]; j = 1, 2 \quad (18)$$

For the temperature dependence of the diffusion coefficient for the diffusion of a water proton away from a Eu^{II} complex, D_{EuH}, we assume a exponential-temperature dependence, with an activation energy E_{DEuH} [Eq. (19)].

$$D_{EuH} = D_{EuH}^{298}\exp\left\{\frac{E_{DEuH}}{R}\left(\frac{1}{T}-\frac{1}{298.15}\right)\right\} \quad (19)$$

Acknowledgements

We kindly acknowledge the support from the Swiss National Science Foundation and the Office for Education and Science (OFES) for financial support. This research was carried out in the frame of the EC COST Action D18.

[1] U. Prinz, U. Englert, U. Koelle, S. Ulrich, A. E. Merbach, O. Maas, K. Hegetschweiler, unpublished results.
[2] R. D. Shannon, *Acta Crystallogr. Sect. A* **1976**, *32*, 751.
[3] R. A. Dwek, R. E. Richards, K. G. Moralee, E. Nieboer, R. J. P. Williams, A. V. Xavier, *Eur. J. Biochem.* **1971**, *21*, 204.
[4] R. B. Lauffer, *Chem. Rev.* **1987**, *87*, 901.
[5] P. Caravan, J. J. Ellison, T. J. McMurry, R. B. Lauffer, *Chem. Rev.* **1999**, *29*, 2293 and references cited therein.
[6] S. Aime, M. Botta, E. Gianolio, E. Terreno, *Angew. Chem.* **2000**, *112*, 763; *Angew. Chem. Int. Ed.* **2000**, *39*, 747.
[7] P. Caravan, A. E. Merbach, *Chem. Commun.* **1997**, 2147.
[8] P. Caravan, É. Tóth, A. Rockenbauer, A. E. Merbach, *J. Am. Chem. Soc.* **1999**, *121*, 10403.
[9] S. Seibig, É. Tóth, A. E. Merbach, *J. Am. Chem. Soc.* **2000**, *122*, 5822.
[10] D. A. Johnson, *Adv. Inorg. Chem. Radiochem.* **1977**, *20*, 1 and references cited therein.
[11] E. J. Onstott, *J. Am. Chem. Soc.* **1952**, *74*, 3773.
[12] X.-T. Fu, C.-M. Wang, Y.-X. Zhang, *Anal. Chim. Acta* **1993**, *272*, 221.
[13] J. C. Barnes, P. A. Bristow, *Inorg. Nucl. Chem. Letters* **1969**, *5*, 565.
[14] G. Laurenczy, E. Brücher, *Proc. Int. Symp. Rare Earth Spectr.* Wroclaw, **1984**, 127.
[15] U. Böttger, O. Galin, H. Schumann, M. Michman, *Inorg. Chim. Acta* **1995**, *231*, 29.
[16] E. L. Yee, O. A. Gansow, M. J. Weaver, *J. Am. Chem. Soc.* **1980**, *102*, 2278.
[17] M. C. Almasio, F. Arnaud-Neu, M. J. Schwing-Weill, *Helv. Chim. Acta* **1983**, *66*, 1296.
[18] J. Jiang, N. Higashiyama, K. Machida, G. Adachi, *Coord. Chem. Rev.* **1998**, *170*, 1.
[19] C. A. Chang, M. E. Rowland, *Inorg. Chem.* **1983**, *22*, 3866.
[20] R. Delgado, J. J. R. F. da Silva, M. C. T. A. Vaz, P. Paoletti, M. Micheloni, *J. Chem. Soc. Dalton Trans.* **1989**, 133.
[21] E. Brücher, B. Györi, J. Emri, S. Jakab, P. Solymosi, I. Tóth, *J. Chem. Soc. Dalton Trans.* **1995**, 3353.
[22] H. Gries, H. Miklautz, *Physiol. Chem. Phys. Med. NMR* **1984**, *16*, 105.
[23] D. M. Pfund, J. G. Darab, J. L. Fulton, Y. Ma, *J. Phys. Chem.* **1994**, *98*, 13102.
[24] R. Ruloff, T. Gelbrich, E. Hoyer, J. Sieler, L. Beyer, *Z. Naturforsch.* **1998**, *53b*, 955.
[25] T. Uechi, J. Ueda, M. Tazaki, M. Takagi, K. Ueno, *Acta Crystallogr. Sect. B* **1982**, *38*, 433.
[26] H. D. Powell, O. M. Ni Dhubhghaill, D. Pubanz, Y. S. Lebedev, W. Schlaepfer, A. E. Merbach, *J. Am. Chem. Soc.* **1996**, *118*, 9333.
[27] C. Cossy, L. Helm, A. E. Merbach, *Inorg. Chem.* **1989**, *28*, 2699.
[28] S. F. Lincoln, A. E. Merbach, *Adv. Inorg. Chem.* **1995**, *42*, 1.
[29] Z. Otwinowski, W. Minor in *Methods in Enzymology*, *Vol. 276*: *Macromolecular Crystallography*, *Part A* (Eds.: C. W. Jr. Carter, R. M. Sweet), Academic Press, **1997**, pp. 307–326.
[30] J. W. Plugrath, *Acta Crystallogr. Sect. D* **1999**, *55*, 1718.
[31] Molecular Structure Corporation, New Trails Drive The Woodlands, Texas, 77381–5209, USA, **1998**.
[32] G. M. Sheldrick, *Acta Crystallogr. Sect. A* **1990**, *46*, 467.
[33] Bruker AXS, Inc., Madison, Wisconsin, 53719, USA, 1997.
[34] H. M. Irving, M. G. Miles, L. D. Petit, *Anal. Chim. Acta* **1967**, *38*, 475.
[35] A. D. Hugi, L. Helm, A. E. Merbach, *Helv. Chim. Acta* **1985**, *68*, 508.
[36] R. V. Vold, J. S. Waugh, M. P. Klein, D. E. Phelps, *J. Chem. Phys.* **1968**, *48*, 3831.
[37] S. Meiboom, D. Gill, *Rev. Sci. Instrum.* **1958**, *29*, 688.
[38] U. Frey, L. Helm, A. E. Merbach, *High Press. Res.* **1990**, *2*, 237.
[39] L. Zékány and I. Nagypál in *Computational Methods for Determination of Formation Constants* (Ed.: D. J. Leggett), Plenum, New York, **1985**, p. 291.
[40] A. D. McLachlan, *Proc. R. Soc. London A* **1964**, *280*, 271.
[41] D. H. Powell, A. E. Merbach, G. González, E. Brücher, K. Micskei, M. F. Ottaviani, K. Köhler, A. von Zelewsky, O. Y. Grinberg, Y. S. Lebedev, *Helv. Chim. Acta* **1993**, *76*, 2129.

Received: March 14, 2000 [F2366]

